Journal of Statistical Physics, Vol. 72, Nos. 3/4, 1993

The Tricritical Behavior of Self-Interacting Partially Directed Walks

A. L. Owczarek,[1] T. Prellberg,[1] and R. Brak[1]

Received December 22, 1992; final April 7, 1993

We present the thermodynamics of two variations of the interacting partially directed self-avoiding walk problem by discussing versions where the length of the walks assume real as well as a integral values. While the discrete model has been considered previously to varying degrees of success, the continuous model we now define has not. The examination of the continuous model leads to the *exact* derivation of several exponents. For the discrete model some of these exponents can be calculated using a continued-fraction representation. For both models the crossover exponent ϕ is found to be 2/3. Moreover, we confirm the tricritical nature of the collapse transition in the generalized ensemble and calculate the full scaling form of the generating function. Additionally, the similarities noticed previously to other models, but left unexplored, are explained with the aid of necklacing arguments.

KEY WORDS: Tricritical point; directed walk; exact solution; q-series.

1. INTRODUCTION

There has been much interest in partially directed self-avoiding walks (PDSAW) as free walks,[1] with self-interactions,[2–4] as interacting with a surface,[5,6] and combining both self- and surface potentials.[7–9] The great virtue of these models, as a simplification of the isotropic self-avoiding walk family of models, is that many analytic techniques can be applied. The behavior of free or noninteracting PDSAW has been understood[1] in great details and the relevant "critical" exponents and scaling functions have been calculated. Critical indices for the model with only surface interactions have also been calculated. However, for the model with only self-interactions, the IPDSAW model, critical exponents have been absent from the

[1] Department of Mathematics, University of Melbourne, Parkville, Victoria 3052, Australia.

0022-4715/93/0800-0737$07.00/0

discussions. This addition of nearest-neighbor monomer–monomer interaction has allowed the study of a model displaying a collapse transition, as occurs in the interacting case of the (undirected) self-avoioding walk (SAW) model. This transition is believed to be a tricritical point in the interacting SAW model and is seen as describing the θ-point of a dilute solution of polymers. The partially directed model has also been seen to possess such a collapse transition.[7] Previous work on the IPDSAW model has located the collapse transition,[2] while other work[3] has calculated the exact generating function of the model and proved the existence of the free energy and the collapse transition. The functions involved in this solution are q-hypergeometric functions for which far less is known about their behavior than standard special functions. As a consequence the calculation of exponents has not yet occurred. In this paper we consider two models, a "discrete" and a "continuous" IPDSAW as illustrated in Fig. 1. Our major results include the values for the common exponents at the collapse transition given in Table II. In Section 2 we provide a broad sketch of the behavior of the models, define these relevant exponents, and present the consequences of the tricritical scaling expected. By solving *exactly* the continuous IPDSAW model, whose generating function can be written in terms of Bessel functions, we are able to study their asymptotics and hence extract the critical exponents (Section 3). As a bonus we calculate the scaling form of the generating function. A new continued-fraction representation of the solution to the discrete models is obtained (Section 4) and we generalize the solution (Appendix A) to include variables needed for a finer study of the problem. Assuming that certain exponents exist enables us to use the continued-fraction representation to calculate several of these exponents. The values obtained are the same as those found more rigorously in the continuous model. We show that the continuous model is the continuum limit (Section 5) of the discrete model and are therefore able to understand the equality of the exponents in some detail. Lastly (Section 6) we explain how both the discrete and our new continuous version of the IPDSAW model are related to other models in the literature. In particular, the models of polymer crystallization of Zwanzig and Lauritzen (ZL) and the two-dimensional linear solid-on-solid (SOS) in a magnetic field are shown by using necklacing arguments to be directly related to our models.

2. SCALING

In this paper we examine two very similar models. The first is defined by considering a two-dimensional square lattice and choosing one vertex of that lattice from which to begin. From that vertex one builds partially

directed self-avoiding walks of varying lengths, as in Fig. 1. Our problem in statistical mechanics is the construction of the partition function $Q_L(T)$ in the canonical ensemble of fixed length L walks where we have nearest-neighbor (attractive) monomer–monomer interactions. The canonical partition function for the model is given by

$$Q_L(T) = \sum_m c_m^{(L)} \exp(mJ/k_B T) \tag{2.1}$$

where $-J$ is the energy associated with each nearest-neighbor contact, $c_m^{(L)}$ is the number of configurations with L steps and m nearest-neighbor contacts, and k_B is Boltzmann's constant. The interactions introduce the temperature and despite later generalizations the partition function is essentially a function of this one variable. A variation on this model is obtained if we consider a slightly different set of configurations and this gives us our second model. Here we allow the vertical segment length to assume real values and the interaction strength between successive vertical "folds" to depend solely on the overlap of the two (in analogy with the discrete model). This model can be conceived as the short-step limit of the discrete one. The two models behave in a similar fashion, as one might expect. The thermodynamic limit in these problems is the limit $L \to \infty$. We now discuss the critical exponents with which we are concerned. For convenience they are summarized in Fig. 2. In the case of infinite temperature or no interactions (free walks) the thermodynamic limit is often referred to as a critical point. The terminology and the subsequent definition of the free walk exponents have been influenced by the formal equivalence of free isotropic SAW and the $n \to 0$ limit of the $O(n)$ model. The most common exponents are the partition function exponent γ and the

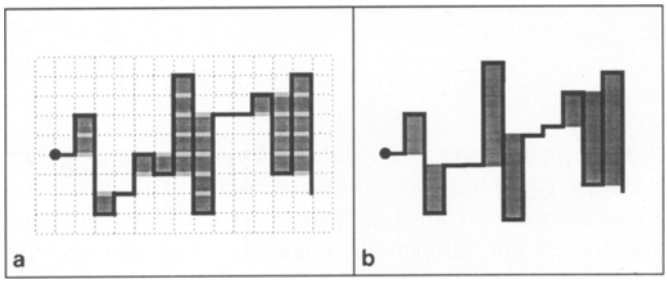

Fig. 1. (a) A typical configuration of a discrete IPDSAW with interaction bonds shaded gray. (b) A typical configuration of a continuous IPDSAW with interaction overlap shown dark gray.

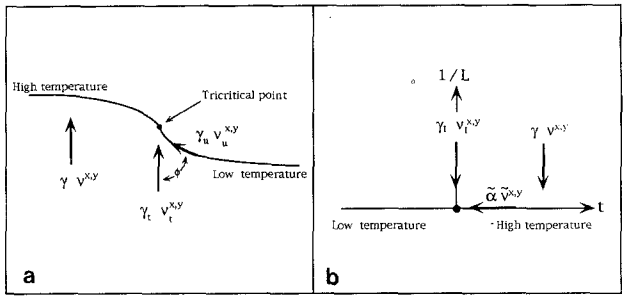

Fig. 2. Diagrams illustrating the critical exponents and the associated limit directions (a) in the singularity diagram or generalized ensemble and (b) in the canonical ensemble.

length scale exponent ν. The exponent γ is defined through the expected scaling form of the partition function as

$$Q_L \sim \mu^L L^{\gamma-1}, \qquad T=\infty \tag{2.2}$$

and has the value $\gamma=1$ in PDSAW. Because this is a directed problem, there are two length scale exponents that can be defined, each measuring essentially the average size of walks in the horizontal, $\nu^x=1$, and vertical directions, $\nu^y=1/2$. These exponents are defined via the radius of gyration $\langle\langle (R^{x,y})^2 \rangle\rangle^{1/2}(L)$, itself being an average (denoted by $\langle\langle \cdot \rangle\rangle$) over the configurations of length L, as

$$\langle\langle (R^{x,y})^2 \rangle\rangle^{1/2} \sim L^{\nu^{x,y}} \tag{2.3}$$

By adding interactions to the problem, and hence a temperature, there exists scope not only for analysis of a large-L scaling behavior, but also of fully thermodynamic phenomena. One goal is then the solution of the limiting free energy per step/monomer

$$f_\infty(T) = -k_b T \lim_{L\to\infty} \frac{1}{L} \log Q_L(T)$$

This function of (real) temperture contains (usually) a lone singularity, that is, there exists a (thermodynamic) critical point. The phase transition is interpreted as a collapse transition where the dominant configurations at high temperatures are elongated, relatively thin though rough, that "collapse" under stronger interactions (lower temperatures) to rather fatter ones. A set of canonical critical point exponents is defined at the singular point. In addition to the thermodynamic limit, the limiting behavior itself is of interest in physics as in the case of free walks. The set of finite-length

scaling exponents takes on three different values, depending on the temperature, one at high temperatures, one at the critical point (T_c), and another in the collapsed phase. As one may expect, the high-temperature values are identical to those of free walks.

It is difficult, however, to sum directly the partition function for fixed lengths and so an alternate route is usually followed. A generating function $G(T, z) = \sum z^L Q_L(T)$ is calculated instead. This can be viewed as simply a mathematical device, being a Laplace transform of a kind or as the physical consideration of a new ensemble. This ensemble, referred to as a generalized ensemble because it has no independent parameter that is varied to produce the thermodynamic limit, is one of a single polymer chain in contact with a particle bath of monomers. The resulting "phase" diagram (or more precisely a singularity diagram) in the z–T plane (see Fig. 3) is summarized as follows. At any temperature there exist values of z small enough that the generating function converges. The generating function has a radius of convergence $0 < z_\infty(T)$ for all temperature (given that the thermodynamic free energy exists). The radius of convergence is in fact related to the thermodynamic free energy as

$$z_\infty(T) = \exp[\beta f_\infty(T)] \tag{2.4}$$

Thus the shape of the radius of convergence gives directly information about the canonical free energy and hence some of the critical point exponents. The thermodynamic limit in the generalized ensemble can be

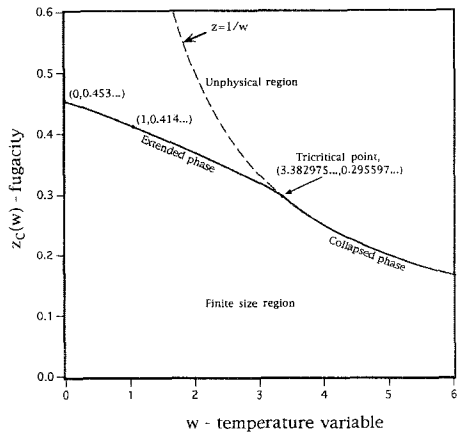

Fig. 3. The singularity diagram for the discrete IPDSAW model. Points whose coordinates were previously known exactly are shown. This diagram has been calculated from the continued-fraction expansion described in Section 4. The singularity diagram for the continuous model is similar.

taken as the limit $z \to z_\infty(T)$ as long as the generating function diverges smoothly as the limit is taken.[10] This condition is fulfilled at temperatures down to and including the collapse temperature. Under these conditions and in the thermodynamic limit averages in the canonical ensemble converge to the same value as the same property averaged in the generalized ensemble. Moreover, the strength of the singularity of the limit itself (as measured canonically by the finite length exponents) in both ensembles can be simply related. Hence, the exponents γ and $\nu^{x,y}$ can be calculated in the generalized (also referred to as a grand in some of the literature) ensemble rather than directly from the (canonical) definitions above. Let us examine this so-called phase diagram further. First, the region $z > z_\infty$ is not of interest usually, even though by suitably extending the problem (by introducing a finite lattice and hence a volume parameter) the radius of convergence may be interpreted as a phase boundary in the z–T plane. Below $z_\infty(T)$ the average walk length is finite (as calculated in the generalized ensemble). At high temperatures and also at the critical temperature the average walk length diverges on approaching the radius of convergence. One may expect this, of course, if the canonical limit $L \to \infty$ is equivalent to the limit $z \to z_\infty(T)$. At low temperatures the average walk length stays finite at $z_\infty(T)$. It is expected that at low temperatures there exists an essential singularity on $z_\infty(T)$ in analogy with the Fisher description of the condensation of a fluid.[11] The low-temperature line is then analogous to a line of first-order transitions. In the same vein the "critical" point can be seen to be analogous to a tricritical point in the $z - T$ plane. In fact, a tricritical point is precisely what is expected at the collapse transition (or θ-point) of polymer systems. It is this tricritical point that will be the focus of our study. We shall refer to the thermodynamic critical point or collapse transition at T_c as a tricritical point and indeed see that the crossover phenomenon associated with such a point does occur in our models.

We shall now define the exponents that characterize the tricritical point. In anticipation of our results, we describe the scaling picture that is expected at the collapse transition using the assumption of conventional tricritical scaling. It is the calculation of these exponents and confirmation of this scaling picture that form the kernel of this paper.

The most common canonical exponents calculated at the (tri-)critical point are $\tilde{\alpha}$ and $\tilde{\nu}^{x,y}$ (x and y denote the horizontal and vertical directions, respectively). The $\tilde{\alpha}$ exponent desibes the singular part of the free energy near T_c as

$$f_\infty^{\text{singular part}}(T) \sim t^{2-\tilde{\alpha}} \tag{2.5}$$

where $t = T - T_c$. The $\tilde{\nu}$ exponents are defined through an appropriate thermal correlation length as

$$\xi^{x,y} \sim t^{-\tilde{\nu}^{x,y}} \tag{2.6}$$

Please note the use of tildes to differentiate these (canonical) thermodynamic exponents from the length scaling exponents.

One can define the finite length scaling exponents γ and $\nu^{x,y}$ via the partition function and the horizontal/vertical radius of gyration at any temperature in the same fashion as in the infinite-temperature case. Three separate values of these exponents are possible, depending on the temperature, and we denote the high-temperature values simply with the same symbols as the free walk definitions, while we denote the tricritical point values by the addition of the subscript t, such as γ_t. The exponents at high temperatures and at the tricritical point can also be calculated using the generalized ensemble and so we give the appropriate definitions used in this ensemble. (Strictly speaking, we should use different symbols for these *a priori*.) The new set of γ exponents is defined through the divergence of the generating function (since the partition function and generating functions are related via the Laplace-like transform) as

$$G(z, T) \sim \Delta z^{-\gamma} \tag{2.7}$$

at high temperatures, where $\Delta z = z_\infty - z$, and

$$G(z, T) \sim \Delta z^{-\gamma_t} \tag{2.8}$$

at T_c. The radius-of-gyration exponents are defined through the average horizontal/vertical length calculated in the generalized ensemble (these averages are denoted $\langle \cdot \rangle$). We have

$$\langle L_{x,y} \rangle \sim \Delta z^{-\nu^{x,y}} \tag{2.9}$$

at high temperatures, and by adding the subscript t a similar equation denotes the tricritical definition. (Here $\langle L_y \rangle$ is the average vertical length of a single vertical segment, rather than the average number of vertical steps, whereas $\langle L_x \rangle$ is the average number of horizontal steps.) The above formulas are easier to tally with the previous definitions when it is realized that the existence of the exponent γ ensures the following behavior:

$$\langle L \rangle \sim \Delta z^{-1} \tag{2.10}$$

for the average total length $\langle L \rangle$.

The generalized canonical exponent ψ describing the singularity of the shape of the radius of convergence can be related to $\tilde{\alpha}$, the exponent of the singular part of the free energy (2.5) through the relationship (2.4). We clearly have

$$\psi = 2 - \tilde{\alpha} \tag{2.11}$$

In addition, the generalized canonical exponents $\nu_u^{x,y}$, measured approaching T_c along the radius of convergence, are expected to reproduce the values of the canonical $\tilde{\nu}^{x,y}$ respectively, since above T_c the calculation of quantities such as a thermal correlation length will result in identical results in the two ensembles.[10] These could be found then by calculating a two-point correlation function as in Nordholm's work.[10] We choose to calculate these exponents by considering the average length scales $\langle L_{x,y} \rangle$ in the grand ensemble (assuming the existence of only a single length scale in the problem near T_c), approaching the tricritical point sitting at the radius of convergence *below* T_c. These averages converge at the radius of convergence when $T < T_c$. This simpler method has been chosen to illustrate the power of the generalized ensemble even below T_c. (Our results are in agreement with Nordholm's method.)

The description of the collapse transition in the generalized ensemble can be given succinctly with the assumption of the transition point being a generic tricritical point. This allows us to write the scaling form, for positive t,

$$G(\Delta z, t) \sim \Delta z^{-\gamma_t} \Theta(\Delta z^{-1} t^{1/\phi}) \tag{2.12}$$

where

$$\Theta(x) \sim \begin{cases} (x - x_c)^{-\gamma}, & x \to x_c \\ \text{const}, & x \to 0 \end{cases} \tag{2.13}$$

where x_c is related to the radius of convergence. This introduces the *crossover* exponent ϕ. Contained in our assumption is the relationship

$$\psi = 1/\phi \tag{2.14}$$

(Please note that this definition of ϕ deviates from the conventional tricritical usage where it is defined so that $\phi = \psi$, but is chosen here to coincide with that most common in the literature concerning the θ-point.) Considering a similar scaling form for the length scale exponents gives $\phi = \nu_t^x \nu_u^x = \nu_t^y / \nu_u^y$. Making an analogous assumption for negative t adjusted for the fact that the generating function does not diverge on the radius of

convergence (given that if exponents exist on this side they will be the same as their positive t counterparts), we have

$$G(t) \sim t^{-\gamma_u} \tag{2.15}$$

where $\gamma_u = \gamma_t/\phi$. (The exponent γ_u can be also found in a *tangential* high-temperature approach along the phase boundary to the tricritical point.)

This scaling assumption has consequence for the scaling of the free energy and partition function in the canonical ensemble. Without going into detail, since we do not use the canonical ensemble for calculation, scaling forms may be written down using basic crossover forms where there is a single crossover exponent ϕ and the relationship $2-\tilde{\alpha}=1/\phi$ is automaticaly satisfied.

The above summary has defined the major exponents discussed in the following sections and sets the scene for the calculation of these exponents and the scaling function defined in (2.12). The more general consideration of the tricritical scaling assumption in walk-type problems has been discussed by Owczarek *et al.*[12] and Brak *et al.*[13] In addition, there exists a recent numerical study of the collapse phase by Prellberg *et al.*[14]

3. CONTINUOUS IPDSAW

In this section we analyze a continuous version of the IPDSAW problem. The great virtue of this approach is the neat and direct calculation of exponents and scaling functions. While the discrete model has been examined in other publications, this is the first place the continuous version has been considered. The rewards for doing so flow the fact that the solution is expressed in terms of Bessel functions whose asymptotics have been well studied. The occurrence of Bessel/q-Bessel functions in problems where the configurations are the continuous/discrete directed walk problems seems generic. We begin by discussing the definition of the model and the various partition and generating functions of interest.

The configurations of the continuous IPDSAW are partially directed walks where the length of each vertical segment is allowed to assume real values. Such a freedom would be natural when considering a model for short monomer polymers (and so a walk model with short step length) and also in a course-grained formulation of the original discrete model. This leads to the examination of the limiting process that would result in our continuous model (starting with the discrete case) and forms the crux of Section 5. Note that because of the directed nature of the problem the continuous model is noticeably asymmetrical (the horizontal length, being made of single steps, can be made to vanish in the continuous limit). Alter-

natively, since the horizontal and vertical limits are decoupled, one is also able to consider a continuum limit where the horizontal step length remains finite, as is done in this paper. Instead, we introduce a dummy variable to count the number of vertical segments, which is numerically equal to the number of horizontal steps (whatever their length).

We assign an energy $U(r_1,..., r_N)$ to each configuration of length L and number of vertical segments N, where each vertical segment, $i = 1,..., N$, has length r_i measured in the positive y direction, giving $L = \sum_{i=1}^{N} |r_i|$. This energy is given by

$$U(r_1,..., r_N) = -J \sum_{i=1}^{N-1} u(r_i, r_{i+1}) \tag{3.1}$$

where

$$u(r_i, r_{i+1}) = \min(|r_i|, |r_{i+1}|)\, \mathscr{H}(-r_i r_{i+1}) \tag{3.2}$$

and $\mathscr{H}(r)$ is the Heaviside step function:

$$\mathscr{H}(r) = \begin{cases} 0, & r < 0 \\ 1/2, & r = 0 \\ 1, & 1 > 0 \end{cases} \tag{3.3}$$

The function $u(r_i, r_{i+1})$ measures the overlap of successive segments. This model differs from the ZL model in that successive segments need not fold back at each horizontal step, hence the complication of the Heaviside function in the energy. We consider the case of attractive monomer–monomer interactions where $J \geqslant 0$. The thermodynamics can be deduced from the canonical partition function

$$Q_L(\omega) = \sum_{N=1}^{\infty} \int_{-\infty}^{\infty} dr_1 \cdots \int_{-\infty}^{\infty} dr_N\, \delta\left(\sum_{i=1}^{N} |r_i| - L \right) \omega^{\sum_i u(r_i, r_{i+1})} \tag{3.4}$$

where the Dirac delta function restricts the "counting" to fixed-length (equal to L) walks and $\omega = \exp(\beta J) \geqslant 1$. The free energy in the thermodynamic (long-walk) limit is defined in the usual way as

$$f(\omega) = -k_B T \lim_{L \to \infty} \frac{1}{L} \log Q_L(\omega) \tag{3.5}$$

For mathematical convenience, then, it is easier to work in the generalized ensemble of fixed monomer fugacity y (so that the length is now allowed to vary). To this end we define the generalized partition function as

$$G(y; \omega) = \int_0^{\infty} y^L Q_L(\omega)\, dL \tag{3.6}$$

This is the Laplace transform of the partition function and therefore can be inverted if required, provided the usual conditions apply. We will, however, calculate thermodynamic averages in the generalized ensemble, although noting the restrictions pointed out by Nordholm.[10] For small enough y the generalized partition function is finite. Interest lies in the radius of convergence $y_\infty(\omega)$ of this function, since this is directly related to the free energy via

$$f(\omega) = k_B T \log y_\infty(\omega) \tag{3.7}$$

The variable y is conjugate to the length and so plays the required role of providing information indirectly about the finite-length scaling.

We now perform some manipulations similar to those that led to a solution in the discrete model. By interchanging the summation and integration, $G(y; \omega)$ can be rewritten as

$$G(y; \omega) = \sum_{N=1}^{\infty} Z_N(y; \omega) \tag{3.8}$$

where

$$Z_N(y; \omega) = \int_{-\infty}^{\infty} dr_1 \cdots \int_{-\infty}^{\infty} dr_N \, e^{-\beta E[r_i]} \tag{3.9}$$

and

$$-\beta E[r_i] = -\tau \sum_{i=1}^{N} |r_i| + \beta J \sum_{i=1}^{N-1} u(r_i, r_{i+1}) \tag{3.10}$$

where $\tau > 0$ and is defined through $y = \exp(-\tau) < 1$. As an aside, we note that if the local interaction $u(r_i, r_{i+1})$ were an absolute difference, then the energy would be that of a solid-on-solid (SOS) model with a magnetic field term. The generalized partition function $G(y; \omega)$ as a function of the temperature (interaction energy) $\omega \geqslant 1$ and fugacity $y < 1$ is the goal of solution. We extend our aim (with a view to obtaining extra detail in the solution) by the introduction of a counting variable $x \leqslant 1$ for the number of folds (or horizontal steps)

$$G(x, y; \omega) = \sum_{N=1}^{\infty} x^N Z_N(y; \omega) \tag{3.11}$$

We also now introduce the function $\mathscr{Z}_N(z)$, which is defined fully as

$$\mathscr{Z}_N(z) = \int_{-\infty}^{\infty} dt \exp[-\tau |t| + \beta J \min(|t|, |z|) \mathscr{H}(-tz)] \, \mathscr{Z}_{N-1}(t) \tag{3.12}$$

and

$$\mathscr{Z}_0(z) = 1 \tag{3.13}$$

Hence

$$Z_N(y; \omega) = \mathscr{Z}_N(0) \tag{3.14}$$

We will therefore be interested in finding $G(x, y; \omega)$ via the generating function $\mathscr{G}(z)$, where

$$\mathscr{G}(z) = \sum_{N=1}^{\infty} x^N \mathscr{Z}_N(z) \tag{3.15}$$

and hence

$$G(x, y; \omega) = \mathscr{G}(0) \tag{3.16}$$

To find the generating function, we find an integral equation which $\mathscr{G}$ satisfies. The integral equation is reduced (with loss of boundary condition) to a differential equation. The solution to the differential equation is then substituted back into the integral equation to fix the constants of the differential equation's general solution. Finally, $z = 0$ is substituted into the solution to find $G(x, y; \omega)$. The method is closely related to the solution of the discrete case and one can view $\mathscr{G}(z)$ as related to the generating function for continuous walks where the first vertical segment is of length z. To find the required integral equation, the recursive formula for $\mathscr{Z}_N(z)$ is substituted into the equation for $\mathscr{G}(z)$. The summation and integration are interchanged, resulting in

$$\mathscr{G}(z) = x \int_{-\infty}^{\infty} dt \{\exp[-\tau|t| + \beta J \min(|t|, |z|)\, \mathscr{H}(-tz)]\}[\mathscr{G}(t) + 1] \tag{3.17}$$

This equation is valid for all real z. The function $\mathscr{G}(z)$ is even, so we need consider only the half-line $[0, \infty)$. Splitting the range of integration about zero and then expressing the result as a single integral on the half-line [using the even property of $\mathscr{G}(z)$], we can reformulate the integral equation as

$$\mathscr{G}(z) = x \int_{0}^{\infty} dt \{\exp(-\tau t) + \exp[-\tau t + \beta J \min(t, |z|)]\}[\mathscr{G}(t) + 1] \tag{3.18}$$

The $\min(\cdot)$ function can be rewritten in terms of sums and differences; that is,

$$\min(x, y) = \tfrac{1}{2}(x + y) - \tfrac{1}{2}|x - y| \tag{3.19}$$

and so by multiplying by $\exp(-\beta Jz/2)$ we obtain

$$\mathscr{F}(z) = e^{-Kz}\mathscr{G}(z) = \int_0^\infty dt\, e^{-Ht}(e^{-K(t+z)} + e^{-K|t-z|})[\mathscr{F}(t) + e^{-Kt}] \tag{3.20}$$

where

$$K = \frac{\beta J}{2} \tag{3.21}$$

and

$$H = \tau - \beta J \tag{3.22}$$

Differentiating this integral equation results in the following differential equation:

$$\frac{d^2\mathscr{F}}{dz^2} = K^2\mathscr{F}(z) - 2Kxe^{-Hz}[\mathscr{F}(z) + e^{-Kz}] \tag{3.23}$$

We preempt Section 6 by remarking that the differential equation above also occurs in the work of Zwanzig and Lauritzen, even though the integral equation (and hence the solution) does not appear. It is convenient to make the substitutions

$$u = ae^{-Hz/2} \tag{3.24}$$

where

$$a^2 = \frac{8Kx}{H^2} \tag{3.25}$$

and

$$F(u) = \mathscr{F}(z(u)) \tag{3.26}$$

to give

$$u^2\frac{d^2F}{du^2} + u\frac{dF}{du} + (u^2 - \lambda^2)F(u) = \frac{-u^{2+\lambda}}{a^\lambda} \tag{3.27}$$

where

$$\lambda = 2K/H \tag{3.28}$$

This is an inhomogeneous form of Bessel's differential equation. The general solution can be written down immediately as

$$F(u) = \frac{-u^\lambda}{a^\lambda} + C_1J_\lambda(u) + C_2J_{-\lambda}(u) \tag{3.29}$$

This solution is then substituted back into the integral equation to determine the constants. By equating orders, the constant C_2 is seen to vanish and the remaining constant is given by

$$C_1 = \frac{aH}{4xJ'_\lambda(a)} \tag{3.30}$$

so that the complete solution is

$$1 + \mathscr{G}(z) = \frac{aHe^{Kz}J_\lambda(ae^{-Kz})}{4xJ'_\lambda(a)} \tag{3.31}$$

Simply substituting $z = 0$ allows us to express the full solution as

$$1 + G(x, y; \omega) = \sigma^{-1}\frac{J_\lambda(\sigma\lambda)}{J'_\lambda(\sigma\lambda)} \tag{3.32}$$

where

$$\sigma = \left(\frac{4x}{\beta J}\right)^{1/2} \tag{3.33}$$

and, reiterating,

$$\lambda = \frac{\beta J}{\tau - \beta J} \tag{3.34}$$

while $\omega = e^{\beta J}$ and $y = e^{-\tau}$.

The expression has been derived assuming $\lambda \geqslant 0$ or $\tau \geqslant \beta J$, which translates to $y \leqslant \omega^{-1}$. The ratio of the two Bessel functions is meromorphic and diverges at the zeros of the denominator. Note that $\sigma = \sigma(x, \omega)$ and $\lambda = \lambda(y, \omega)$, so that the counting variable and the length fugacity play asymmetric roles. Quantities of interest are first the generalized partition function itself

$$G(y; \omega) = G(1, y; \omega) \tag{3.35}$$

which is found simply by using $\sigma = \sigma(1, \omega)$ without changing the order λ of the Bessel function. The average number of segments is given by

$$\langle N \rangle = \left.\frac{\partial \log G(x, y; \omega)}{\partial \log x}\right|_{x=1} \tag{3.36}$$

and the average length by

$$\langle L \rangle = \frac{\partial \log G(1, y; \omega)}{\partial \log y} \tag{3.37}$$

The radius of convergence $y_\infty(\omega)$, and so the free energy, can be found implicitly. The generalized partition function $G(y;\omega)$ diverges when

$$J'_\lambda(\sigma\lambda)=0 \tag{3.38}$$

and the solutions to this equation depend crucially on whether σ is less than or greater than one. In fact, the condition $\sigma=1$ or

$$\beta_c J=4 \tag{3.39}$$

describes the critical point in the system. For a given high temperature such that $\sigma(\omega)>1$ there exists a smallest (nonzero) finite positive solution of (3.38) for λ or (translating) a solution for $y=y_\infty(\omega)$ in the interval $(0,\omega^{-1})$. If the temperature considered changes and approaches that defined by the condition (3.39), then the solution λ approaches infinity and $y_\infty(\omega)\to\omega^{-1}$. For low temperatures, $\sigma(\omega)<1$, the generating function converges for all $y\in[0,\omega^{-1}]$. There is an infinite sequence of poles above ω^{-1} that accumulates there, hence $y_\infty(\omega)=\omega^{-1}$ for $\omega\geqslant\omega_c$.

Our rewards are now at hand. The generalized partition function can be seen to have a isolated pole singularity for high temperatures, so the standard exponent $\gamma=1$. Below the critical temperature the generalized canonical γ does not exist, which implies that the standard ansatz for the asymptotics of the partition function (in L) does not hold in the canonical ensemble. At the critical temperature $\gamma_t=1/3$. We note again that $\langle L\rangle$ diverges with a simple pole provided γ exists. In fact, it is possible to write down the complete scaling form around the critical temperature for the generalized partition function as

$$G(y(\lambda);\omega(\zeta))\approx -\left(\frac{\zeta}{1-\sigma^2}\right)^{1/2}\frac{\mathrm{Ai}(\lambda^{2/3}\zeta)}{\mathrm{Ai}'(\lambda^{2/3}\zeta)}\lambda^{1/3} \tag{3.40}$$

where $\zeta(\sigma)$, the temperature scaling variable, is defined differently above and below the critical point as

$$\frac{2}{3}\zeta^{3/2}=\log\frac{1+(1-\sigma^2)^{1/2}}{\sigma}-(1-\sigma^2)^{1/2} \tag{3.41}$$

for $\sigma<1$ and

$$\frac{2}{3}(-\zeta)^{3/2}=(\sigma^2-1)^{1/2}-\arccos\left(\frac{1}{\sigma}\right) \tag{3.42}$$

for $\sigma>1$. Note that

$$|\zeta|\sim|1-\sigma^2|\sim|T-T_c| \tag{3.43}$$

for $\sigma \approx 1$ and that

$$|\lambda| \sim \frac{1}{|y_\infty(\omega_c) - y|} \tag{3.44}$$

for $y \approx y_\infty(\omega_c)$ and $\sigma \approx 1$. The differing high- and low-temperature definitions of ζ hint at the underlying gross asymmetry in the collapse transition physically. This can be clearly seen from the free energy: in the collapsed phase (low temperature) the free energy is a constant (hence the entropy is zero!), while above the critical temperature the free energy has a well-defined singular variation. The approximation above has the tricritical scaling form mentioned previously. From this scaling expression the crossover exponent $\phi = 2/3$ is simply extracted. This is consistent with the divergence of the generating function on approaching the critical temperature from below fixed at the radius of convergence $y_\infty(\omega) = \omega^{-1}$, since, for $\omega > \omega_c$,

$$G(y_\infty; \omega) \sim (\omega - \omega_c)^{-1/2} \tag{3.45}$$

which confirms $\gamma_u = \gamma_t/\phi = 1/2$. The average number of segments, which is equal to the number (not length of) the horizontal steps, is given by

$$\langle N \rangle = \frac{\sigma\lambda[J'_\lambda(\sigma\lambda)/J_\lambda(\sigma\lambda) - (\sigma^{-2} - 1)\, J_\lambda(\sigma\lambda)/J'_\lambda(\sigma\lambda)]}{2[1 - \sigma J'_\lambda(\sigma\lambda)/J_\lambda(\sigma\lambda)]} \tag{3.46}$$

Even though N is strictly not a length, we use it to define a horizontal scale and in turn an exponent ν^x. Nordholm defines a true correlation length which produces identical results for the ZL model. This quantity diverges on approaching y_∞ for high temperatures with a simple pole, so we assign

$$\nu^x = 1 \tag{3.47}$$

whereas at the critical temperature

$$\nu_t^x = 2/3 \tag{3.48}$$

found from (3.46). Again this agrees with the crossover scaling expectation for the exponent

$$\nu_u^x = 1 = \nu_t^x/\phi \tag{3.49}$$

The shape of the radius of convergence curve, which defines the exponent ψ and is found independently from analysis of (3.28), gives $\psi = 3/2$. This is consistent with is consistent with the hypothesis of general

Table I. High-Temperature Exponents

Exponent	γ	ν^x	ν^y
Value	1	1	1/2

tricritical scaling, which demands $\psi = 1/\phi$. As mentioned in the previous section, utilizing the fact that the radius of convergence curve is the curve is the plot of the free energy, the canonical specific heat exponent is

$$\tilde{\alpha} \equiv 2 - \psi = 1/2 \tag{3.50}$$

All these exponents agree, as we shall see, with those that can be found, making some scaling assumptions, from the discrete model. A complete set of exponents set of exponents can be deduced,[2] including

$$\nu_t^y = 1/3 \tag{3.51}$$

and

$$\nu_u^y = 1/2 \tag{3.52}$$

(Remembering that using arguments found in Nordholm's paper,[10] we have $\tilde{\nu}^{x,y} = \nu_u^{x,y}$.)

It is then worthwhile to note that the normal hyperscaling is satisfied at the tricritical point

$$\tilde{\nu}^x + \tilde{\nu}^y = 2 - \tilde{\alpha} \tag{3.53}$$

since the equation, also satisfied,

$$2 - \tilde{\alpha} = 1/\phi \tag{3.54}$$

is believed can be understood as a "fractal" hyperscaling relation. This exponent relation has been discussed recently in work on the general assumption of tricritical points.

We now summarize our values for the exponents in Tables I and II.

[2] Foster has subsequently calculated ν_t^x and ν_t^y.[15]

Table II. Tricritical Exponents

Exponent	γ_t	ν_t^x	ν_t^y	γ_u	ν_u^x	ν_u^y	$\tilde{\alpha}$	ϕ	ψ
Value	1/3	2/3	1/3	1/2	1	1/2	1/2	2/3	3/2

4. DISCRETE MODEL

Here we describe and analyze the discrete IPDSAW model. Although this model has been solved previously,[3] much has been added to the understanding of the solution itself. In particular, a deeper analysis of the properties of q-Bessel functions leads to the understanding of the critical behavior of the model.

We start with the description of the model and present a solution within the generalized canonical ensemble. The existence of a singularity in the free energy as a function of the interaction energy in the thermodynamic limit and hence a phase transition are shown. Then, utilizing a continued-fraction expansion of the solution, analyticity properties of the generating function are proved and the structure of the critical point is investigated. In particular, we compute the exponents of the associated tricritical scaling form.

The configurations of this model are partially directed walks on a two-dimensional square lattice with nearest-neighbor interactions. For later convenience, we demand that these walks end with a horizontal segment. Due to the directed nature of this problem, we can describe these configurations in a natural way through the length r_i of vertical segments between two horizontal steps, measured in the positive y direction. Thus, we associated to each configuration an N-tuple $(r_1, r_2, ..., r_N)$ corresponding to a configuration of total length $L = \sum_{i=1}^{N} |r_i| + N$.

The energy due to the nearest-neighbor interactions for each of these configurations is then

$$U(r_1, r_2, ..., r_N) = -Ju(r_1, r_2, ..., r_N) \tag{4.1}$$

where

$$u(r_1, r_2, ..., r_N) = \sum_{i=1}^{N-1} \min(|r_i|, |r_{i+1}|)\, \mathscr{H}(-r_i r_{i-1}) \tag{4.2}$$

We assign weights x for steps in the horizontal direction and y for steps in the vertical direction. The canonical partition function as a sum over all possible configurations of fixed length L is then

$$Q_L(x, y, \omega) = \sum_{N=1}^{L} x^N \sum_{|r_1| + |r_2| + \cdots + |r_N| = L - N} y^{L-N} \omega^{u(r_1, r_2, ..., r_N)} \tag{4.3}$$

where we have set $\omega = \exp(\beta J)$. We get the generalized partition function by summing over all possible lengths,

$$\begin{aligned} G(x, y, \omega) &= \sum_{L=1}^{\infty} Q_L(x, y, \omega) \\ &= \sum_{N=1}^{\infty} x^N \sum_{M=0}^{\infty} y^M \sum_{|r_1| + |r_2| + \cdots + |r_N| = M} \omega^{u(r_1, r_2, ..., r_N)} \end{aligned} \tag{4.4}$$

so that we have

$$Q_L(x, y, \omega) = [z^L] G(zx, zy, \omega) = \frac{1}{2\pi i} \oint G(zx, zy, \omega) \frac{dz}{z^{L+1}} \tag{4.5}$$

In the Appendix, we consider a generalization of this model which differentiates between steps into the positive and negative y directions and thus allows for, e.g., the modeling of an external field.

In order to derive an expresion for $G(x, y, \omega)$, consider now the generalized partition functions $G_r = G_r(x, y, \omega)$ for walks that start with a vertical segment of height r, so that

$$G(x, y, \omega) = \sum_{r=-\infty}^{\infty} G_r \tag{4.6}$$

Then we can concatenate these walks to get a recursion relation for G_r as follows:

$$G_r = xy^{|r|} \left\{ 1 + \sum_{s=-\infty}^{\infty} \omega^{u(r,s)} G_s \right\} \tag{4.7}$$

It follows that

$$G_0 = x\{1 + G(x, y, z)\} \tag{4.8}$$

Using the symmetry $G_r = G_{-r}$ and then restricting to $r \geqslant 0$, we can further simplify to

$$G_r = xy^r \left\{ 1 + \sum_{s=0}^{\infty} G_s + \sum_{s=1}^{\infty} \omega^{\min(r,s)} G_s \right\} \tag{4.9}$$

which will be the starting point of our investigation.

We will now derive a homogeneous second-order difference equation which we can solve using an ansatz from ref. 1. Using the scaling behavior of the solutions, we can eliminate one of the two linearly independent solutions. We then write the general solution of (4.9) as an expression involving the quotient of two q-hypergeometric functions.

Taking differences in (4.9), we first eliminate the inhomogeneous term,

$$G_{r+1} - yG_r = xq^{r+1} \left(1 - \frac{1}{\omega}\right) \sum_{s=r+1}^{\infty} G_s \tag{4.10}$$

Here we introduced for convenience the new variable $q = y\omega$. Upon taking differences a second time, we are left with

$$(G_{r+2} - yG_{r+1}) - q(G_{r+1} - yG_r) = -xq^{r+2} \left(1 - \frac{1}{\omega}\right) G_{r+1} \tag{4.11}$$

In the case of no interaction ($\omega = 1$), the right-hand side of this equation is zero and we have a simple homogeneous difference equation with constant coefficients. Its characteristic polynomial $P(\lambda)$ is

$$P(\lambda) = (\lambda - y)(\lambda - q) \tag{4.12}$$

and the solution is given by $G_r = A_1 y^r + A_2 q^r$.

This motivates the ansatz[1]

$$G_r = \lambda^r \sum_{n=0}^{\infty} q^{nr} c_n \tag{4.13}$$

with $c_n = c_n(x, q, \omega)$ independent of r, which inserted into (4.11) gives

$$P(\lambda) c_0 + \sum_{n=1}^{\infty} q^{nr} \left[P(\lambda q^n) c_n + xq \left(1 - \frac{1}{\omega}\right) \lambda q^n c_{n-1} \right] = 0 \tag{4.14}$$

This equation is solved by

$$P(\lambda) = 0, \qquad \text{i.e.,} \quad \lambda_1 = y \quad \text{and} \quad \lambda_2 = q \tag{4.15}$$

and, choosing $c_0 = 1$,

$$c_n = \prod_{m=1}^{n} \frac{-xq(1 - 1/\omega)\, \lambda q^m}{P(\lambda q^m)} = \frac{[-x(1 - 1/\omega)\lambda]^n q^{\binom{n}{2}}}{(\lambda\omega; q)_n (\lambda; q)_n} \tag{4.16}$$

Here we have used the standard notation

$$(x; q)_n = \prod_{m=1}^{n} (1 - xq^{m-1}) \tag{4.17}$$

Defining

$$H(y, q, t) = \sum_{n=0}^{\infty} \frac{q^{\binom{n}{2}} (-t)^n}{(y; q)_n (q; q)_n} \tag{4.18}$$

we now can write the general solution of (4.11) as

$$G_r = A_1 y^r H\left(y, q, x\left(1 - \frac{1}{\omega}\right) q^{1+r}\right) + A_2 q^r H\left(q\omega, q, x\omega\left(1 - \frac{1}{\omega}\right) q^{1+r}\right) \tag{4.19}$$

We remark that the function H is directly related to a basic hypergeometric function[16]

$$H(y, q, t) = {}_1\phi_1(0, y; q, t) \tag{4.20}$$

which can be seen to be a limiting function of ${}_2\phi_1$ and that is the q-deformation of the more familiar hypergeometric function ${}_2F_1$. Analogously, the function H can be understood (apart from some normalizing factors and seen by taking the limit $q \to 1$) as a q generalization of Bessel functions. Furthermore, as will be seen in the following sections, formally taking the continuum limit vertically transforms Eq. (4.11) into Bessel's differential equation. Therefore, the solution above is also related via this second limit to Bessel functions. In this section, the understanding of the singular behavior of H is at the core of deriving the critical exponents.

Returning to the analysis, we see that, for $|q| < 1$, $H(y, q, tq^r)$ is uniformly bounded in r, so that we can write

$$|G_r| \leqslant \text{const} \cdot (q^r + y^r) \tag{4.21}$$

This we insert into (4.9) and, assuming $0 < \omega^2 y < 1 < \omega$, we get

$$\begin{aligned} |G_r| &\leqslant \text{const} \cdot y^r \left[1 + \sum_{s=0}^{r-1} (\omega q)^s + \omega^r \sum_{s=r}^{\infty} q^s \right] \\ &\leqslant \text{const} \cdot y^r [1 + (\omega q)^r] \\ &\leqslant \text{const} \cdot y^r \end{aligned} \tag{4.22}$$

As $H(y, q, tq^r) \to 1$ for $r \to \infty$, we see that in fact $A_2 = 0$. The reason for this is that we obtained the homogeneous difference equation (4.11) by taking differences from (4.9), thus introducing additional solutions.

The boundary conditions for G_0 and G_1 from (4.9) are

$$G_0 = x \left\{ 1 + \sum_{s=0}^{\infty} G_s + \sum_{s=1}^{\infty} G_s \right\} = x\{1 + G(x, y, \omega)\} \tag{4.23}$$

and

$$\begin{aligned} G_1 &= xy \left\{ 1 + \sum_{s=0}^{\infty} G_s + \omega \sum_{s=1}^{\infty} G_s \right\} \\ &= xy \left\{ \frac{1-\omega}{2} + \left(\frac{1-\omega}{2} x + \frac{1+\omega}{2} \right) (1 + G(x, y, \omega)) \right\} \end{aligned} \tag{4.24}$$

so that we can write down the solution for $G(x, y, \omega)$ as

$$1 + G(x, y, \omega) = \frac{1-\omega}{2} \left\{ \frac{G_1}{yG_0} - \left(\frac{1+\omega}{2} + \frac{1-\omega}{2} x \right) \right\}^{-1} \tag{4.25}$$

and, upon inserting the quotient of the q-Bessel functions,

$$\mathscr{H}(y, q, t) = \frac{H(y, q, qt)}{H(y, q, t)} \tag{4.26}$$

we get

$$1 + G(x, y, \omega) = \frac{1-\omega}{2[\mathscr{H}(y, y\omega, xy(\omega-1)) - 1] + (1-\omega)(1-x)} \tag{4.27}$$

We remark that we could have arrived at the same result by immediately inserting the ansatz (4.13) into the recurrence relation (4.9). However, the above approach has the virtue of being more transparent.

In the further analysis of $\mathscr{H}(y, q, t)$ we restrict ourselves to the region $|q| < 1$, but first we note that the q-Bessel functions converge for $|q| > 1$ as well, and that they are related by

$$H(y, q, qt) = H\left(\frac{1}{y}, \frac{1}{q}, \frac{t}{y}\right) \tag{4.28}$$

so that we have

$$\mathscr{H}(y, q, t)\, \mathscr{H}\left(\frac{1}{y}, \frac{1}{q}, \frac{t}{y}\right) = 1 \tag{4.29}$$

However, there is an essential singularity at $q = 1$.

Further functional equations for $H(y, q, t)$ enable us to derive continued-fraction expansions for $\mathscr{H}(y, q, t)$. We have in particular

$$H(y, q, t) - H(y, q, qt) = -\frac{t}{1-y} H(qy, q, qt) \tag{4.30}$$

$$H(y, q, t) - H(qy, q, t) = -\frac{ty}{(1-y)(1-qy)} H(q^2 y, q, qt) \tag{4.31}$$

$$H(y, q, t) - H(qy, q, qt) = -\frac{t}{(1-y)(1-qy)} H(q^2 y, q, qt) \tag{4.32}$$

so that with defining

$$\tilde{\mathscr{H}}(y, q, t) = \frac{H(qy, q, qt)}{H(y, q, t)} \tag{4.33}$$

we get

$$\mathscr{H}(y, q, t) = 1 - \frac{t}{1-y} \tilde{\mathscr{H}}(y, q, t) \tag{4.34}$$

and

$$\tilde{\mathscr{H}}(y, q, t)=\left\{1-\frac{t}{(1-y)(1-qy)}\left[1-\frac{q^2yt}{(1-qy)(1-q^2y)}\tilde{\mathscr{H}}(q^2y, q, qt)\right]^{-1}\right\}^{-1} \tag{4.35}$$

which defines a (Stieltjes type) continued-fraction expansion for $\tilde{\mathscr{H}}$. Utilizing theorems in Section 54 of ref. 17, we see that for $|q| \neq 1$ this expansion converges to a meromorphic function in t in the whole complex plane. Moreover, the convergence is uniform in any domain excluding the poles of this function. As the continued fraction converges uniformly in a neighborhood of the origin, it is equal to its power series expansion.

Note that the expansion (4.35) is fundamentally different from the continued fraction given in ref. 18. In particular, it has the advantage of having a much larger domain of convergence, and thus facilitates numerical computations of the generating function for all $|q| \neq 1$ (with much better convergence when compared to series expansions). The continued fraction has been used in the computation of the phase diagram in Fig. 3. Also, all exponents given below can be calculated numerically using this expansion.

The above results do not include $q=1$; however, in this case (4.35) yields a simple quadratic equation for $\tilde{\mathscr{H}}(y, 1, t)$, giving rise to square root branch points at $t^2-2(1+y)t+(1-y)^2=0$.

As we will use the continued-fraction expansion given by (4.35) for our further analysis, it is convenient to express (4.27) in terms of $\tilde{\mathscr{H}}$,

$$1+G(x, y, \omega)=\frac{1-y}{(1-x)(1-y)-2xy\tilde{\mathscr{H}}(y, y\omega, xy(\omega-1))} \tag{4.36}$$

in a way suggestive of the singularity structure needed to discuss the phase diagram. We only need to discuss the singularity closest to the origin. This will be on the positive real axis, as G is a power series with positive coefficients. There are two ways for this singularity of G to arise. First, G can have a pole, corresponding to a zero in the denominator, i.e., we have

$$2xy\tilde{\mathscr{H}}(y, y\omega, xy(\omega-1))=(1-x)(1-y) \tag{4.37}$$

From the continued-fraction expansion it is clear that the locus of these zeros depends analytically on ω, as long as $y\omega=q<1$. Second, if there is no zero of (4.37) for $y\omega<1$, then the closest singularity is given by the essential singularity of $\tilde{\mathscr{H}}$ at $y\omega=q=1$. On this line, we can insert $\tilde{\mathscr{H}}(y, 1, x(1-y))$ into (4.37) and see that the two singularities coincide precisely at the square root branch point of that solution, given by

$\omega_c(x, y)$. For $\omega < \omega_c$ we have a simple pole singularity and for $\omega > \omega_c$ we have an essential singularity (G attains in fact a finite value). For more details see ref. 18.

Now we proceed to the calculation of the exponents. First, we note that the square root branch point gives an exponent of $\gamma_u = 1/2$. The central problem in the computations of the exponents away from the line $q = 1$ is that we can get explicit expressions for $\tilde{\mathscr{H}}$, and thus for G, *only* on the line $q = 1$. However, we can compute partial derivatives of all orders on $q = 1$ by differentiating (4.35) and inserting $\tilde{\mathscr{H}}(y, 1, q)$. Thus, we can deduce information about the critical structure from their divergences as $\omega \to \omega_c$ from above. Due to the structure of (4.35), the computations are rather cumbersome and the derivatives grow rapidly in size, which necessitates the use of a symbolic manipulation program. In what follows, we therefore refrain from stating explicit equations.

Due to the existence of all higher-order derivatives on the line $q = 1$, we are justified in writing an asymptotic series expansion of $\tilde{\mathscr{H}}$ in $\varepsilon = 1 - q$, i.e.,

$$\tilde{\mathscr{H}}(y, 1-\varepsilon, t) \sim \sum_{n=0}^{\infty} \tilde{\mathscr{H}}^{(n)}(y, t)\varepsilon^n \tag{4.38}$$

Inserting this equation into (4.35), multiplying out, and sorting by powers of ε yields an iteration scheme for $\tilde{\mathscr{H}}^{(n)}(y, t)$. This iteration scheme shows in particular that in the neighborhood of the branch point $\tilde{\mathscr{H}}^{(n)}(y, t)$ diverges with exponent

$$\gamma_u^{(n)} = \gamma_u + n\Delta \qquad \text{with} \quad \gamma_u = \tfrac{1}{2} \quad \text{and} \quad \Delta = \tfrac{3}{2} \tag{4.39}$$

This "gap exponent" Δ is consistent with a tricritical scaling ansatz which links Δ to the crossover exponent ϕ as

$$\phi = \frac{1}{\Delta} = \frac{2}{3} \tag{4.40}$$

Now consider the computation of γ_t, i.e., the divergence of $G(x, y, \omega_c)$ for $y \to 1/\omega_c$. It can be shown that

$$\frac{\partial G}{\partial y} G^{-4} \bigg|_{\omega = \omega_c,\, y = 1/\omega_c} \tag{4.41}$$

has a finite value. Assuming that the exponent exists, we therefore get

$$(-\gamma_t - 1) + 4\gamma_t = 0 \qquad \text{and thus} \quad \gamma_t = \tfrac{1}{3} \tag{4.42}$$

This independent confirms the above value of the crossover exponent

$$\phi = \frac{\gamma_t}{\gamma_u} = \frac{2}{3} \tag{4.43}$$

A slightly more indirect approach leads to the computation of the shape exponent $\psi = 2 - \alpha$. For this, we compute the shape of the level lines $y_l(\omega)$ from $G(x, y_l(\omega), \omega) = l$ at $y_l(\omega) = 1/\omega$ and then let $l \to \infty$. Analysis of these results shows that $\psi = 3/2$, which confirms $\psi = 1/\phi$.

Therefore, by making an asymptotic expansion and relating this to tricritical scaling, we are able to calculate exactly the rational values of the exponents at the θ-point.

5. CONTINUUM LIMIT

The continuous model and the discrete model can be directly related by taking the continuum limit. If the size of the edges of the lattice, a, are put explicitly into the equations of the discrete model and the limit $a \to 0$ is taken, then the continuous model is obtained. (In order to obtain the continuous model, only the lattice constant in the vertical direction must be allowed to shrink.) Before taking this limit it is necessary to determine the length dimensions of the objects occurring in the equations. As noted in Section 3, $\mathscr{G}(z)$ is the generating function of the partition function $\mathscr{Z}_N(z)$, but it is equally valid to interpret it as a generalized (or grand) partition function for continuous walks whose first vertical step has length z. Thus

$$\frac{\mathscr{G}(z)}{\mathscr{N}}\, dz = \text{probability the first vertical step has length between } z \text{ and } z + dz \tag{5.1}$$

where $\mathscr{N} = \int_0^\infty \mathscr{G}(z)\, dz$. As probabilities are dimensionless, it is consistent for $\mathscr{G}(z)$ to have the dimensions of inverse length. This in turn means that the Boltzmann factors xy^z have the dimensions of inverse length (which, for convenience, we associated with the x factor).

Returning to the discrete model and Eq. (4.9), we make the change of variable from G_r to $\mathscr{G}_r$, where

$$G_r = xy^r(\mathscr{G}_r + 1) \tag{5.2}$$

With this change Eq. (4.9) becomes

$$\mathscr{G}_r = x\mathscr{G}_0 + x + \sum_{s=1}^{\infty} x(y^s + y^s\omega^{\min(r,s)})(1 + \mathscr{G}_s) \tag{5.3}$$

Now we make the length dimensions explicit by inserting the lattice constant a to give

$$\mathscr{G}_{ar} = ax\mathscr{G}_0 + ax + \sum_{s=1}^{\infty} ax(y^{as} + y^{as}\omega^{\min(ar,as)})(1+\mathscr{G}_{as}) \tag{5.4}$$

Now let the lattice shrink to zero, but ensure that the physical length of the walk remains finite by taking the limit $a \to 0$, with ar and as remaining finite. Thus, $ar \to z$, $as \to t$, and $\sum_{s=1}^{\infty} a \to \int_0^{\infty} dt$, and hence Eq. (5.4) becomes

$$\mathscr{G}_z = \int_0^{\infty} dt\, x(y^t + y^t\omega^{\min(z,t)})(1+\mathscr{G}_t) \tag{5.5}$$

If this is compared with Eq. (3.18) of the continuous model, we see that the same equation is obtained with $y \equiv \exp(-\tau)$, $\omega \equiv \exp(\beta J)$, and $\mathscr{G}_z \equiv \mathscr{G}(z)$. As shown in Section 3, the solution to (5.5) is an expression containing Bessel functions. The same result can be obtained from the discrete solution if the continuum limit is taken after the solution to the recurence relation is obtained. This result demonstrates clearly which expressions in the discrete solution become Bessel functions in the continuum limit.

We begin with the recurrence relation (4.9) and obtain a functional equation as follows. Let

$$S(v) = \sum_{r=1}^{\infty} v^r G_r \tag{5.6}$$

Then, using (4.9), we obtain

$$S(v) = (1+G_0)\frac{xyv}{1-yv} + xS(1)\left(\frac{yv}{1-yv} + \frac{\omega yv}{1-\omega yv}\right)$$
$$+ xS(\omega yv)\left(\frac{yv}{1-yv} - \frac{\omega yv}{1-\omega yv}\right) \tag{5.7}$$

This functional equation can now be solved to give

$$S(v) = x\sum_{n=0}^{\infty} x^n \left\{\frac{yq^n v}{1-yq^n v}[1+G_0+S(1)] + S(1)\frac{q^{n+1}v}{1-q^{n+1}v}\right\}$$
$$\times \prod_{k=1}^{n}\left(\frac{yq^{k-1}v}{1-yq^{k-1}v} - \frac{q^k v}{1-q^k v}\right) \tag{5.8}$$

where $q = \omega y$. Thus, by letting $v = 1$, we obtain

$$S(1) = (1 + \mathscr{G}_0)\, \mathscr{T}(q, y; y) + S(1)[\mathscr{T}(q, y; y) + \mathscr{T}(q, y; q)] \tag{5.9}$$

where

$$\mathscr{T}(q, y; t) = x \sum_{n=0}^{\infty} \frac{x^n t q^n}{1 - t q^n} \prod_{k=1}^{n} \left[\frac{y q^{k-1}}{1 - y q^{k-1}} - \frac{q^k}{1 - q^k} \right] \tag{5.10}$$

and hence

$$S(1) = \frac{(1 + G_0)\, \mathscr{T}(q, y; y)}{1 - \mathscr{T}(q, y; y) - \mathscr{T}(q, y; q)} \tag{5.11}$$

Before taking the continuum limit we once again make the length dimensions explicit by inserting the lattice constant a, to give

$$S^a(1) = \frac{(1 + a G_0)\, \mathscr{T}^a(q, y; y)}{1 - \mathscr{T}^a(q, y; y) - \mathscr{T}^a(q, y; q)} \tag{5.12}$$

with

$$\mathscr{T}^a(q, y; t) = x \sum_{n=0}^{\infty} \frac{a x^n t^a q^{an}}{1 - t^a q^{an}} \prod_{k=1}^{n} \left[\frac{a y^a q^{a(k-1)}}{1 - y^a q^{a(k-1)}} - \frac{a q^{ak}}{1 - q^{ak}} \right] \tag{5.13}$$

Now, taking the limit $a \to 0$ gives the surprisingly simple results

$$\begin{aligned} \lim_{a \to 0} \mathscr{T}^a(q, y; y) &= \Gamma(\lambda) \left(\frac{\sigma \lambda}{2} \right)^{1-\lambda} J_{\lambda+1}(\sigma\lambda) \\ \lim_{a \to 0} \mathscr{T}^a(q, y; q) &= 1 - \Gamma(\lambda) \left(\frac{\sigma \lambda}{2} \right)^{1-\lambda} J_{\lambda-1}(\sigma\lambda) \\ \lim_{a \to 0} S^a(1) &= \frac{J_{\lambda+1}(\sigma\lambda)}{J_{\lambda-1}(\sigma\lambda) - J_{\lambda+1}(\sigma\lambda)} \end{aligned} \tag{5.14}$$

where Γ and J_λ are the gamma function and Bessel functions, respectively, $\sigma = (4x/\beta J)^{1/2}$, and $\lambda = \beta J/(\tau - \beta J)$.

Now, as $G^a(x, y; \omega) := \sum_{r=-\infty}^{\infty} a G_r = a G_0 + 2 S^a(1)$, in the continuum limit we obtain

$$G(x, y; \omega) := \lim_{a \to 0} G^a(x, y; \omega) = \frac{2 J_{\lambda+1}(z)}{J_{\lambda-1}(z) - J_{\lambda+1}(z)} \tag{5.15}$$

and hence, by using Bessel functions identities, we obtain

$$1 + G(x, y; \omega) = \frac{J_\lambda(\sigma\lambda)}{\sigma J'_\lambda(\sigma\lambda)} \tag{5.16}$$

This is precisely the continuum model result [cf. Eq. (3.32)].

6. CONNECTIONS

When the IPDSAW model was studied previously the similarity of the models discussed by Zwanzig and Lauritzen[19,20] to the IPDSAW was noticed. The models can be formally written down in similar fashion and it is clear that due to the different set of configurations considered the models differ somewhat. In this paper we have shown that the exponents are identical where they exist and in fact while solving the continuous version the *same* differential equation occurs. Here we resolve the tantalizing similarities by showing that one set of problems follows from the other, using a necklacing[21] argument.

The major difference between the models is that in the Zwanzig and Lauritzen (ZL) models the configurations are such that at each horizontal step the walk is constrained to fold back onto itself (see Fig. 4). The absence or not of length assigned to the horizontal steps in the continuous versions has been discussed in Section 3 and is not a difference between the ZL and IPDSAW models.

We begin by defining the ZL model at the generalized canonical level. In the continuous version the generating function is given by

$$G(x, y; \omega) = \sum_{N=1}^{\infty} x^N Z_N(y; \omega) \tag{6.1}$$

where

$$Z_N(y; \omega) = \int_0^\infty dr_1 \cdots \int_0^\infty dr_N \, e^{-\beta E[r_i]} \tag{6.2}$$

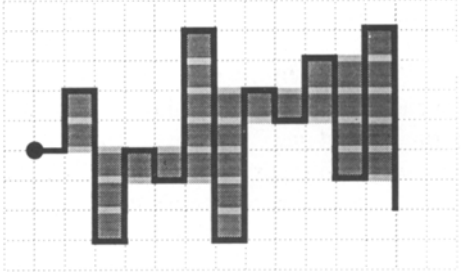

Fig. 4. A typical configuration of a discrete ZL walk with interaction bonds shown light gray.

with

$$-\beta E[r_i] = -\tau \sum_{i=1}^{N} r_i + \beta J \sum_{i=0}^{N-1} u(r_i, r_{i+1}) \tag{6.3}$$

and

$$u(r_i, r_{i+1}) = \min(r_i, r_{i+1}) \tag{6.4}$$

(The lengths r_i are defined to be positive in this model.) The definition is similar to that of the continuous IPDSAW in Section 4 apart from the range of integration in the expression for $Z_N(y;\omega)$ and the absence of the Heaviside function in the energy $u(r_i, r_{i+1})$. The discrete model is defined analogously with the summations substituted for the integrals in the expression for $Z_N(y;\omega)$. Hence, for the discrete model

$$Z_N(y;\omega) = \sum_{r_1=0}^{\infty} \cdots \sum_{r_N=0}^{\infty} e^{-\beta E[r_i]} \tag{6.5}$$

where the energy is given by the same expression as in the continuous case. This has the same relation to the discrete IPDSAW that the continuous model had to its counterpart.

As pointed out in the section on the continuous model, the expression $Z_N(y;\omega)$ is similar to the partition function for the SOS model with magnetic field term. In fact, in the case of the ZL model there is an *exact* correspondence. Rewriting the energy equation (6.3) as

$$-\beta E[r_i] = -H \sum_{i=1}^{N} r_i - K \sum_{i=1}^{N-1} \{r_1 + |r_{i+1} - r_i| + r_N\} \tag{6.6}$$

makes this explicit, where $H = \tau - \beta J$ and $K = \beta J/2$ as defined during the solution of the continuous model. Recently[22] a generating function approach has been applied to the discrete version of the two-dimensional SOS model in a magnetic field with a boundary potential. Without the boundary potential the expression for the generating function is identical to that for the discrete ZL model. In the continuous case also this relationship is manifest in previous work on the ZL [see Eq. (34) of ref. 19] and the SOS models [see Eq. (16) of ref. 23]. These similarities occur because, as we have seen, the energy and partition function of the SOS model with magnetic field (though no excess boundary energy) occur in intermediate stages of the solution to the ZL as defined above. The difference between the problems lies in which variables are considered fugacities: in the SOS model the radius of convergence in x paramount, while in the ZL (and

IPDSAW) it is a dummy variable set to one or y. Because there is a also a difference in the definitions of the lengths r_i themselves, this equivalence cannot be extended to the SOS problem with boundary energy (that is, to be possibly related to the ZL model with boundary potential). (In the SOS model the r_i are the absolute heights of the horizontal steps above some fixed boundary, while in the ZL and IPDSAW they are differences between successive steps.) The IPDSAW model with boundary potential has been investigated elsewhere.[8,9]

The generalized partition function $ZL^{\text{cont}}(x, y; \omega)$ for the continuous ZL model is

$$1 + ZL^{\text{cont}}(x, y; \omega) = 2\sigma^{-1} \frac{J_\lambda(\sigma\lambda)}{J_{\lambda-1}(\sigma\lambda)} \tag{6.7}$$

where, repeating for convenience,

$$\sigma = \left(\frac{4x}{\log \omega}\right)^{1/2} \tag{6.8}$$

and

$$\lambda = \frac{\log \omega}{\log y^{-1} - \log \omega} \tag{6.9}$$

The generalized partition function $ZL^{\text{disc}}(x, y; \omega)$ for the discrete ZL model is

$$1 + ZL^{\text{disc}}(x, y; \omega) = \frac{1-\omega}{H(x, x\omega, xy^2\omega(\omega-1))/H(x, x\omega, xy(\omega-1)) + 1 - (1+\omega) - (1-\omega)x} \tag{6.10}$$

where the q-Bessel function $H(x, q, t)$ is defined as before:

$$H(x, q, t) = \sum_{n=0}^{\infty} \frac{q^{\binom{n}{2}}(-t)^n}{(x; q)_n (q; q)_n} \tag{6.11}$$

with

$$(x; q)_n = \prod_{m=1}^{n} (1 - xq^{m-1}) \tag{6.12}$$

One can compare these to the results of the previous sections, where we now denote the generalized partition functions by $PD(x, y; \omega)$:

$$1 + PD^{\text{cont}}(x, y; \omega) = \sigma^{-1} \frac{J_\lambda(\sigma\lambda)}{J'_\lambda(\sigma\lambda)} \tag{6.13}$$

for the continuous IPDSAW, and for the discrete IPDSAW is given by

$$1 + PD^{\text{disc}}(x, y; \omega) = \frac{1-\omega}{2[H(x, x\omega, xy^2\omega(\omega-1))/H(x, x\omega, xy(\omega-1))] - (1+\omega) - (1-\omega)x} \tag{6.14}$$

The argument linking the ZL and IPDSAW models is slightly different in the continuous and discrete cases, so let us begin with the simpler, which is the continuous version. The essence of the argument is understanding how to construct configurations of the IPDSAW model from the restricted ZL space of walks. The energies of the common configurations are identical (suitably chosen); in fact, the ZL configurations form a subset of the full IPDSAW space. Consider an arbitrary IPDSAW walk. One can see that this walk can be uniquely partitioned into ZL subwalks concatenated together (see Fig. 5). Remember that ZL walks are those with at least one vertical segment, and one horizontal step is attached to each segment. By considering other IPDSAWs it is not difficult to convince oneself that any IPDSAW walk can be found by concatenating a certain number of ZL walks. Moreover, the set of walks obtained by concatenating ZL walks together, taking account of the arbitrariness of the direction of the first vertical segment, is precisely the set of IPDSAW configurations. The generating function can be constructed likewise as

$$PD^{\text{cont}}(x, y; \omega) = 2ZL^{\text{cont}}(x, y; \omega) \sum_{k=0}^{\infty} [ZL^{\text{cont}}(x, y; \omega)]^k \tag{6.15}$$

so

$$PD^{\text{cont}}(x, y; \omega) = \frac{2ZL^{\text{cont}}(x, y; \omega)}{1 - ZL^{\text{cont}}(x, y; \omega)} \tag{6.16}$$

The expressions given above satisfy this relationship.

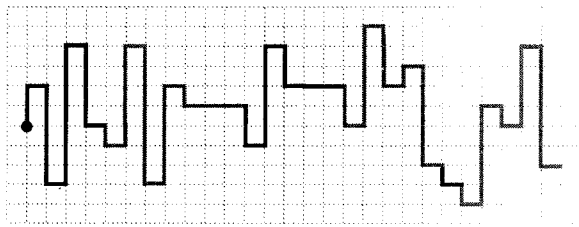

Fig. 5. A typical discrete IPDSAW walk showing how it can be uniquely decomposed into ZL walks.

The discrete case is complicated by the fact that one must avoid double counting those walks that begin with a horizontal step. Moreover, in the construction of the IPDSAW configurations from ZL walks each building block must take this double counting into consideration. This results in using

$$ZL(x, y; \omega) - x[1 + ZL(x, y; \omega)] \tag{6.17}$$

instead of simply $ZL(x, y; \omega)$ as the building block generating function. Again the IPDSAW generating function is constructed as

$$PD^{\text{disc}}(x, y; \omega) = [2ZL^{\text{disc}} - x(1 + ZL^{\text{disc}})] \times \sum_{k=0}^{\infty} [ZL^{\text{disc}} - x(1 + ZL^{\text{disc}})]^k \tag{6.18}$$

giving

$$PD^{\text{disc}}(x, y; \omega) = \frac{2ZL^{\text{disc}}(x, y; \omega) - x[1 + ZL^{\text{disc}}(x, y; \omega)]}{1 - \{ZL^{\text{disc}}(x, y; \omega) - x[1 + ZL^{\text{disc}}(x, y; \omega)]\}} \tag{6.19}$$

Again this relationship is easily verified using the exact expressions for the discrete generating functions. The necklacing arguments link the ZL and IPDSAW problems, while the ZL solution formally contains a certain SOS model solution. These connections account for the appearance of the same functions as solutions to several different problems considered in the literature.

APPENDIX. THE GENERALIZATION OF THE DISCRETE MODEL

One step toward the computation of the length-scale exponents of IPDSAW is to distinguish between vertical segments, depending on their orientation in the walk. This leads to the investigation of a four-variable generating function of the discrete model.

Although this generalization is still solvable, the solution is in the form of a rather complex expression. Nonetheless, this is an interesting generalization of the difference equations in Section 4.

We introduce y_+ and y_- as variables conjugate to steps into the positive y and negative y directions, respectively. Writing $G_r^+ = G_r$ and $G_r^- = G_{-r}$ for nonnegative r (i.e., $G_0^+ = G_0^-$), we get in straightforward analogy to (4.9)

$$G_r^{\pm} = xy_{\pm}^r \left\{1 + \sum_{s=0}^{\infty} G_s^{\pm} + \sum_{s=1}^{\infty} \omega^{\min(r,s)} G_s^{\mp}\right\} \tag{A.1}$$

This leads to the following difference equation:

$$(G^{\pm}_{r+2} - y_{\pm} G^{\pm}_{r+1}) - q_{\pm}(G^{\pm}_{r+1} - y_{\pm} G^{\pm}_{r}) = -x q_{\pm}^{r+2}\left(1 - \frac{1}{\omega}\right) G^{\mp}_{r+1} \tag{A.2}$$

where we denote $q_{\pm} = \omega y_{\pm}$.

In the case of no interaction ($\omega = 1$), the right-hand side of this equation is again zero and we have a set of decoupled homogeneous difference equations with constant coefficients.

For $\omega \neq 1$, however, we now have to solve a set of coupled difference equations. For this it is convenient to introduce vector notation. Defining

$$\mathbf{G}_r = \begin{pmatrix} y_+^{-r} G_r^+ \\ y_-^{-r} G_r^- \end{pmatrix} \tag{A.3}$$

and the off-diagonal matrix

$$\Omega_r = \begin{pmatrix} 0 & q_+^r \\ q_-^r & 0 \end{pmatrix} \tag{A.4}$$

we can write (A.2) as

$$(\mathbf{G}_{r+2} - \mathbf{G}_{r+1}) - \omega(\mathbf{G}_{r+1} - \mathbf{G}_r) = -x(\omega - 1)\Omega_{r+1}\mathbf{G}_{r+1} \tag{A.5}$$

The characteristic polynomial for the lhs of (A.5) is

$$P[\lambda] = (\lambda - 1)(\lambda - \omega) \tag{A.6}$$

For later convenience, we also define

$$\Gamma = \begin{pmatrix} q_+ & 0 \\ 0 & q_- \end{pmatrix} \tag{A.7}$$

In modification of (4.143), we try the ansatz

$$\mathbf{G}_r = \lambda^r \sum_{n=0}^{\infty} \Omega_r^n \mathbf{c}_n \qquad \text{with} \quad \mathbf{c}_n = \begin{pmatrix} c_r^+ \\ c_r^- \end{pmatrix} \tag{A.8}$$

which leads to

$$P[\lambda]\mathbf{c}_0 + \sum_{n=1}^{\infty} \Omega_r^n \{(\lambda^2 \Omega_r^{-n} \Omega_{r+2}^n - (1+\omega)\lambda \Omega_r^{-n}\Omega_{r+1}^n + \omega I)\mathbf{c}_n + x(\omega - 1)\lambda \Omega_r^{-n}\Omega_{r+1}^n \mathbf{c}_{n-1}\} = 0 \tag{A.9}$$

where I is the 2×2 identity matrix. It is due to the appearance of matrix products in this equation that the solution is more complicated. Fortunately, these matrix products simplify, as

$$\Omega_r^{-2m}\Omega_{r+s}^{2m}=(q_+q_-)^{sm} \quad \text{and} \quad \Omega_r^{1-2m}\Omega_{r+s}^{2m-1}=(q_+q_-)^{s(m-1)}\Gamma^s \tag{A.10}$$

Thus, the sum can be split up into even and odd terms,

$$\begin{aligned}0=P[\lambda]\mathbf{c}_0+\sum_{m=1}^{\infty}\Omega_r^{2m}\{P[\lambda(q_+q_-)^m]\mathbf{c}_{2m}+x(\omega-1)\,\lambda(q_+q_-)^m\mathbf{c}_{2m-1}\}\\ +\sum_{m=1}^{\infty}\Omega_r^{2m-1}\{P[\lambda(q_+q_-)^{m-1}\Gamma]\mathbf{c}_{2m-1}+x(\omega-1)\,\lambda(q_+q_-)^{m-1}\Gamma\mathbf{c}_{2m-2}\}\end{aligned} \tag{A.11}$$

Again, we have two solutions $\lambda_0=1$ and $\lambda_1=\omega$. Comparison with Section 4 shows that we have to choose $\lambda_0=1$, as the two solutions have to coincide for $q_-=q_+=q$. Thus

$$c_{2m}^{\pm}=\frac{-x(\omega-1)(q_+q_-)^m}{P[(q_+q_-)^m]}\,c_{2m-1}^{\pm} \quad \text{and} \quad c_{2m+1}^{\pm}=\frac{-x(\omega-1)(q_+q_-)^m q_{\pm}}{P[(q_+q_-)^m q_{\pm}]}\,c_{2m}^{\pm} \tag{A.12}$$

whence it follows that

$$c_{2m}^{\pm}=\frac{x^{2m}(\omega-1)^{2m}(q_+q_-)^{m^2}q_{\pm}^m}{\prod_{k=1}^m P[(q_+q_-)^{k-1}q_{\pm}]\,P[(q_+q_-)^k]}\,c_0^{\pm} \tag{A.13}$$

and

$$c_{2m+1}^{\pm}=\frac{-x^{2m+1}(\omega-1)^{2m+1}(q_+q_-)^{m(m+1)}q_{\pm}^{m+1}}{P[(q_+q_-)^m q_{\pm}]\prod_{k=1}^m P[(q_+q_-)^{k-1}q_{\pm}]\,P[(q_+q_-)^k]}c_0^{\pm} \tag{A.14}$$

Inserting this into the ansatz (A.8), we get

$$\begin{aligned}y_{\pm}^{-r}G_r^{\pm}&=\sum_{m=0}^{\infty}(q_+q_-)^{rm}(c_{2m}^{\pm}+q_{\pm}c_{2m+1}^{\mp})\\&=A_r^{\pm}c_0^{\pm}-B_r^{\mp}c_0^{\mp}\end{aligned} \tag{A.15}$$

with

$$A_r^{\pm}=\sum_{m=0}^{\infty}\frac{x^{2m}(\omega-1)^{2m}(q_+q_-)^{m(m+r)}q_{\pm}^m}{\prod_{k=1}^m P[(q_+q_-)^{k-1}q_{\pm}]\,P[(q_+q_-)^k]} \tag{A.16}$$

$$B_r^{\pm}=\sum_{m=0}^{\infty}\frac{x^{2m+1}(\omega-1)^{2m+1}(q_+q_-)^{m(m+r)}q_{\pm}^{r+m+1}}{P[(q_+q_-)^m q_{\pm}]\prod_{k=1}^m P[(q_+q_-)^{k-1}q_{\pm}]\,P[(q_+q_-)^k]} \tag{A.17}$$

The initial conditions determine the constants $\mathbf{c}_0$. We get, in analogy to (4.25),

$$1+G(x,y_+,y_-,\omega)=\frac{1-\omega}{2}\left\{\mathscr{H}(x,y_+,y_-,\omega)-\left(\frac{1+\omega}{2}+\frac{1-\omega}{2}x\right)\right\}^{-1} \tag{A.18}$$

where

$$\begin{aligned}\mathscr{H}(x,y_+,y_-,\omega)&=\frac{y_+^{-1}G_1^+ + y_-^{-1}G_1^-}{2G_0}\\ &=\frac{(A_0^+ + B_0^+)(A_1^+ - B_1^+)-(A_0^- + B_0^-)(A_1^- - B_1^-)}{(A_0^+ + B_0^+)(A_0^+ - B_0^+)-(A_0^- + B_0^-)(A_0^- - B_0^-)}\end{aligned} \tag{A.19}$$

The distinction between steps up and down thus leads to an expression which takes into account the coupling between those steps, resulting in $A_r^{\pm} \neq B_r^{\pm}$. For $y_+ = y_- = y$ these expressions become equal, and (A.19) reduces to Eq. (4.27).

ACKNOWLEDGMENTS

We thank A. J. Guttmann for enlightening discussions and are grateful to the Australian Research Council for financial support.

REFERENCES

1. V. Privman and N. M. Švrakić, *Directed Models of Polymers, Interfaces, and Clusters: Scaling and Finite-Size Properties* (Lecture Notes in Physics, Vol. 338, Springer-Verlag, Berlin, 1989).
2. P. M. Binder, A. L. Owczarek, A. R. Veal, and J. M. Yeomans, *J. Phys. A* **23**:L975 (1990).
3. R. Brak, A. Guttmann, and S. Whittington, *J. Phys. A* **25**:2437 (1992).
4. D. J. Klein and W. A. Seitz, in *Nonlinear Topics in Ocean Physics*, A. R. Osbourne, ed. (North-Holland, Amsterdam, 1991).
5. V. Privman, G. Forgacs, and H. L. Frisch, *Phys. Rev. B* **37**:9897 (1988).
6. G. Forgacs, V. Privman, and H. L. Frisch, *J. Chem. Phys.* **90**:3339 (1989).
7. A. R. Veal, J. M. Yeomans, and G. Jug, *J. Phys. A* **23**:L109 (1990).
8. D. P. Foster, *J. Phys. A* **23**:L1135 (1990).
9. F. Iglói, *Phys. Rev. A* **43**:3194 (1991).
10. K. Sture Nordholm, *J. Stat. Phys.* **9**:235 (1973).
11. M. E. Fisher, *Physics* **3**:255 (1967).
12. A. L. Owczarek, T. Prellberg, and R. Brak, *Phys. Rev. Lett.* **70**:951–953 (1993).
13. R. Brak, A. L. Owczarek, and T. Prellberg, *J. Phys. A* (1993).
14. T. Prellberg, A. L. Owczarek, R. Brak, and A. J. Guttmann, *Phys. Rev. E* (1993).

15. D. Foster, *Phys. Rev. E* (1993).
16. G. Gasper and M. Rahman, *Basic Hypergeometric Series* (Cambridge University Press, Cambridge, 1990).
17. H. S. Wall, *Analytic Theory of Continued Fractions* (Van Nostrand, New York, 1948), p. 42.
18. R. Brak and A. J. Guttmann, *J. Phys. A* **23**:4581 (1990).
19. R. Zwanzig and J. I. Lauritzen, Jr., *J. Chem. Phys.* **48**:3351 (1968).
20. J. I. Lauritzen, Jr., and R. Zwanzig, *J. Chem. Phys.* **52**:3740 (1970).
21. M. E. Fisher, *J. Stat. Phys.* **34**:667 (1984).
22. A. L. Owczarek and T. Prellberg, *J. Stat. Phys.* **70**:1175–1194 (1993).
23. D. B. Abraham and E. R. Smith, *J. Stat. Phys.* **43**:621 (1986).